

Brief Opinion

Why Do Both Mean Dose and $V_{\geq x}$ Often Predict Normal Tissue Outcomes?

Lawrence B. Marks, MD,^{a,*} Stefan A. Reinsberg, PhD,^b Ellen Yorke, PhD,^c and Vitali Moiseenko, PhD^d

^aDepartment of Radiation Oncology and Lineberger Comprehensive Cancer Center, University of North Carolina School of Medicine, Chapel Hill, North Carolina; ^bDepartment of Physics and Astronomy, University of British Columbia, Vancouver, British Columbia, Canada; ^cDepartment of Medical Physics, Memorial Sloan Kettering Cancer Center, New York, New York; ^dDepartment of Radiation Medicine and Applied Sciences, University of California, San Diego, La Jolla, California

Received March 17, 2022; accepted July 19, 2022

In the Quantitative Analyses of Normal Tissue Effects in the Clinic (QUANTEC), High Dose per Fraction, Hypofractionated Treatment Effects in the Clinic (HyTEC), and Pediatric Normal Tissue Effects in the Clinic (PENTEC) reviews, the mean dose was identified as a reasonable predictor for risk of toxic effects in some normal organs,¹⁻⁵ particularly in organs classically considered to have a parallel-like architecture, such as the lung, liver, and parotid. The utility of the mean dose as a predictive metric is puzzling, because an underlying biological basis is challenging to define. So, why does this work? Superficially, in a group of patients treated in a relatively uniform manner (eg, with respect to dose and beam arrangement), the mean dose may simply be highly correlated with other potentially more biologically logical parameters such as threshold-based metrics (eg, $V_{\geq x}$, the fraction of organ receiving a dose $\geq x$). We herein present an alternative explanation for the association between the mean dose and clinical outcomes based on both (1) the dose-response relationship between local dose and local function and (2) basic geometric principles for modern radiation therapy (RT) beams.

Dose-Response Relationship Between Local Dose and Local Function

For parallel-like organs, it is reasonable to consider that each region functions relatively independently and that changes in global organ function (that manifest as a clinical toxic effect) might be expected to reflect the sum of regional effects (often termed *integrated response*)⁶:

$$\text{Sum regional effects} = \sum_{D=0}^{D_{max}} V_D * \text{Effect}_D,$$

where V_D is the fractional volume at dose D and Effect_D is the degree of local effect at dose D .

If the dose-response function for *regional injury* (ie, Effect_D) is approximately linear within the clinically relevant dose range, it is reasonable to suppose that the sum of regional effects might be fairly well correlated with the mean dose. Inherent to this argument is that volume is a surrogate for function (ie, that different regions of equal size carry equal functional burdens). We recognize that this overall model is certainly simplistic, but we believe it is a useful construct within which to discuss these issues.

Using lung as an example, the regional function dose response with conventional fractionation (assessed using perfusion single-photon emission tomography) is approximately linear in the 10 to 55-Gy range (Fig 1 A), that is, doses received by much of the incidentally irradiated lung.^{7,8} A similar linear response was observed after lung stereotactic body-RT (SBRT),⁹ and in other organs. For

Sources of support: This work was partly supported by the National Cancer Institute through the University of North Carolina Lineberger Comprehensive Cancer Center core grant (P30-CA016086) and by the Memorial Sloan Kettering Comprehensive Cancer Center core grant (P30 CA00874).

Disclosures: none.

*Corresponding author: Lawrence B. Marks, MD; E-mail: marks@med.unc.edu

<https://doi.org/10.1016/j.adro.2022.101039>

2452-1094/© 2022 Published by Elsevier Inc. on behalf of American Society for Radiation Oncology. This is an open access article under the CC BY-NC-ND license (<http://creativecommons.org/licenses/by-nc-nd/4.0/>).



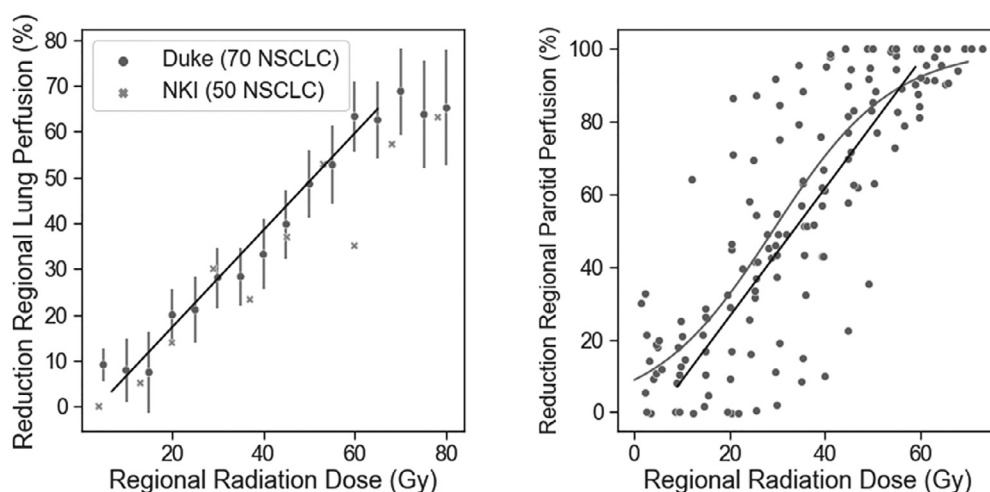


Fig. 1 Dose response curves for regional function. Left: Reductions in regional lung perfusion; data from Duke and Netherlands Cancer Institute (NKI) (based on 70 and 50 patients, respectively, with non-small cell lung cancer). Each data point is the weighted average from multiple regions from multiple patients. Right: Reductions in voxel-specific parotid function estimated by ^{11}C -methionine clearance via positron emission tomography.¹⁰ For both images, the solid line was added to illustrate that the data resemble a linear function. The curved line in the image on the right is from the publication by Buus et al.¹⁰ Adapted with permission from Fried et al.⁶ and Buus et al.¹⁰

parotid, the regional dose response function (assessed using metabolic clearance of ^{11}C -methionine) is noisier, but is approximately linear from 5 to 40 Gy (Fig 1 B).¹⁰ Although the deep parotid is often close to the target (and thus receives approximate target doses of 60-70 Gy), much of the parotid receives lower doses. For the liver, regional portal vein perfusion 1 month after RT declined linearly with local dose.¹¹

Thus, from a physiological perspective, the mean dose is perhaps predictive owing to the approximate linear nature of the dose-response function for regional injury, and since much of the incidental dose is in this region of linearity. In other words, the mean dose is a reasonable surrogate for the integrated response.

Nevertheless, the mean dose is also suboptimal because it ignores *where* dose is delivered (thus, failing to consider possible spatial functional heterogeneities). For example, it has been argued that lung toxic effects are more common in patients receiving RT for lower-lobe tumors.¹² This argument, however, applies both to mean dose and V_x metrics. The mean dose also ignores the general *shape* of the regional dose-response functions that appear to have a threshold (below which there is no injury) and a plateau (above which there is no further injury). Reducing regional doses within regions already at doses less than the threshold or within the plateau region will alter the mean dose but will not affect the integrated response. To lower the integrated response, at least some of the dose reduction has to move regions that are on the plateau or linear regions to lesser doses along the linear or prethreshold regions. Nevertheless, given the uncertainties in these models and imprecision of our normal-tissue toxicity assessments, the ability to predict clinical outcomes based on the mean dose versus the integrated

response are likely similar. The general concept of the threshold and plateau has implications for how one considers competing treatment plans (eg, with 3-dimensional [3D] vs intensity modulated radiation therapy vs proton-based).

In the QUANTEC, HyTEC, and PENTEC reviews, threshold metrics (eg, $V_{\geq x}$, the percentage of the organ receiving a dose $\geq x$) are predictive in several parallel-like organs.¹⁻⁴ From a physiological perspective, this makes sense if we believe there is essentially a step function for regional injury (ie, a steep dose response; regional function ceases above some regionally toxic dose) and one wants to keep some critical organ volume (or fractional volume) below this regionally toxic dose. Given what we know about the often shallow nature of regional dose-response functions,⁷⁻¹⁰ $V_{\geq x}$ metrics are perhaps not logical. Further, the threshold doses sometimes considered for parallel-like organs (eg, $V_{\geq 20}$ for lung) are not consistent with the whole-organ tolerance data (eg, the pulmonary risks after fractionated 20-Gy whole-lung RT appear low; see Fig 3 in the Lung QUANTEC review). Nevertheless, because $V_{\geq x}$ metrics are often correlated with metrics such as the mean dose,^{1,2} they may remain clinically useful. However, this correlation is likely technique dependent, and with evolving and more varied treatment techniques, $V_{\geq x}$ metrics may not be generalizable or transferrable, and the mean dose might be more predictive than $V_{\geq x}$ metrics. Conversely, $V_{\geq x}$ metrics might be more predictive than the mean dose—for example, if the dose-response curve for regional dysfunction is steep and/or the incidental doses received by a meaningful fraction of the organ are outside the region of linearity in the regional dose-response function. In these cases, the mean dose might be predictive for outcomes due to its correlation with $V_{\geq x}$.

Basic Geometric Principles for Modern RT Beams

Interestingly, the degree of correlation between the mean dose and any $V_{\geq x}$ appears to be related to the number of treatment beam orientations used. This concept is illustrated in the idealized 2-dimensional (2D) representation in Figure 2, using area rather than volume. As the number of treatment beam orientations increases, the normal-tissue area receiving low doses increases (the absolute area depends on the organ size; ie, R in Fig 2). Conversely, as the number of beam orientations increases, the area of normal tissue receiving high doses (eg, prescription dose) will decrease (eg, the area of the polygon formed by the intersection of multiple beams decreases). As the number of beam orientations increases

to a high number, the area of the surrounding polygon approaches the target area, thus reducing the normal-tissue area receiving the full prescription dose (this is typical with, and is indeed an essence of, SBRT/stereotactic radio-surgery).

However, the situation at intermediate doses is more complex. For example, consider the area receiving $\geq 1/12$, $\geq 1/6$, or $\geq 1/3$ of a 60-Gy prescription dose (analogous to $V_{\geq 5}$, $V_{\geq 10}$, or $V_{\geq 20}$ for a lung target receiving 60 Gy). The best way to reduce the area receiving one twelfth, one sixth, or one third of the prescription dose is to use >12 , >6 , or >3 beam orientations, respectively. (This is true because the area within the entrance and exit beam path is typically much larger than the area within the regions closer to the target where the treatment beams intersect, because the targets are usually small relative to the total organ volume.) Once these threshold numbers of beam

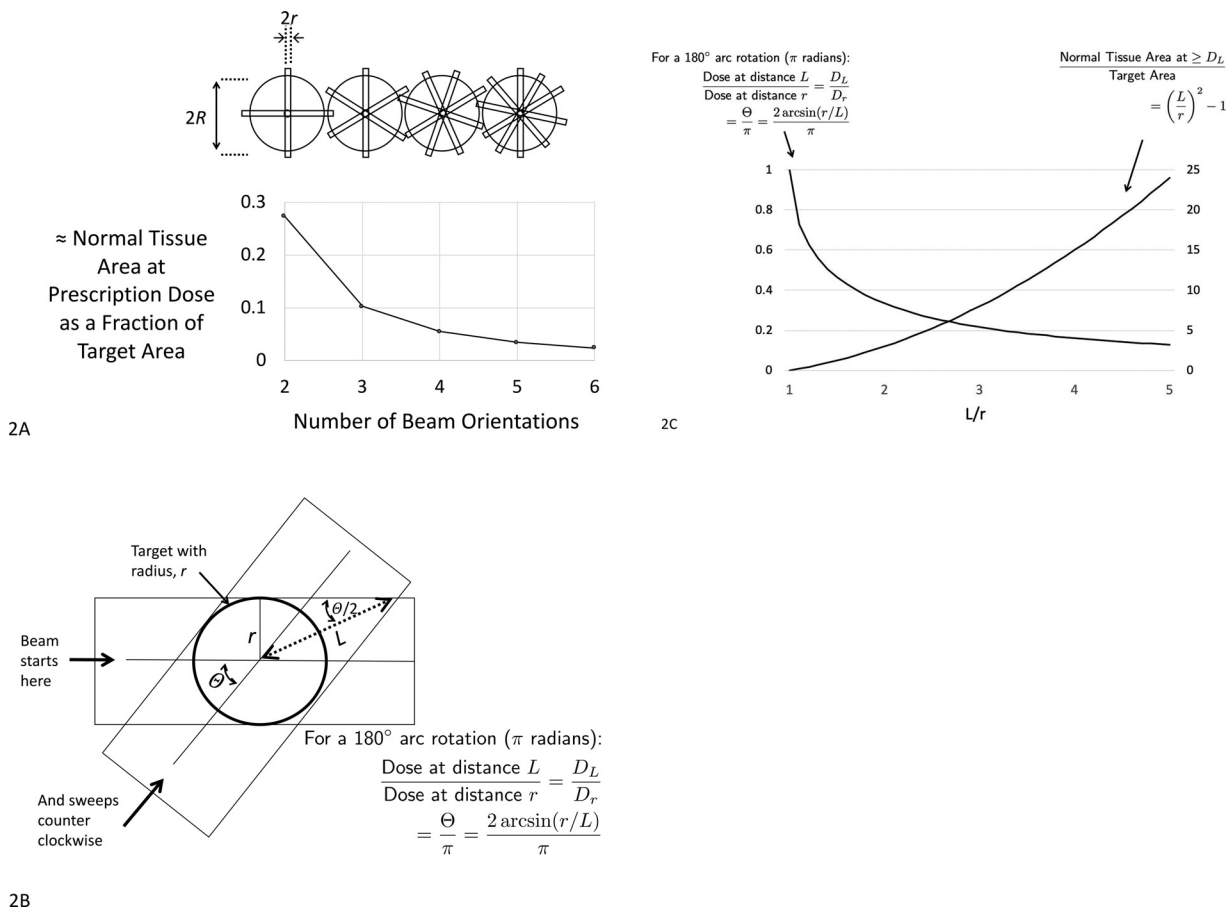
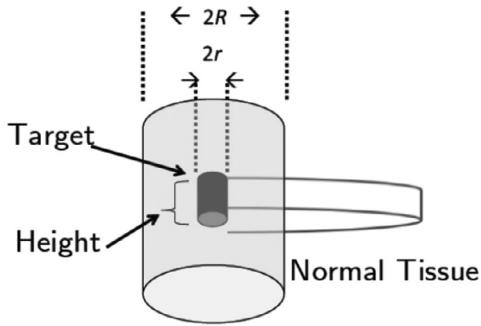


Fig. 2 The idealized 2-dimensional situation of a small circular tumor in a larger circular organ at risk is considered, ignoring effects related to beam divergence and beam attenuation. A, As the number of treatment beam orientations increases, the area of normal tissue receiving a low dose increases, and the absolute area depends on the size of the normal organ (eg, R). As the number of treatment beam orientations increases, the area of normal tissue receiving the full prescription dose decreases approximately as shown (eg, assuming full dose delivered to the area of the regular polygon formed by the intersection of multiple beams surrounding a circular target). B, For an arc rotation, the dose to a point at distance L from the target center (D_L) / dose to the target dose (D_r) = Θ / π . Because $\sin(\Theta/2) = r/L$; $\Theta = 2 \arcsin(D_L/D_r)$, and $D_L/D_r = 2/\pi \times \arcsin(r/L)$. C, For an arc rotation, the isodose lines are circular with the relative doses at variable values of L , and the area receiving doses $\geq D_L$ is computed as shown.

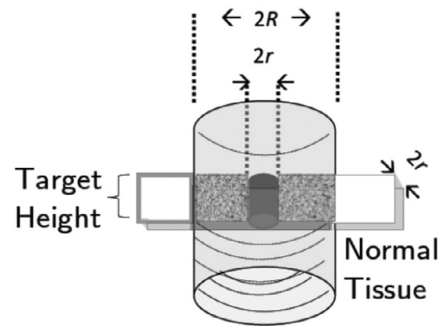
Axial Arc: π radians = 180°



$$V_{D_L} \approx \text{fraction of normal tissue at dose } \geq D_L$$

$$\approx \frac{\pi r^2}{\tan^2(\pi D_L / 2D_r)} \cdot \frac{\text{Target Height}}{\text{Normal Tissue Volume}}$$

Single Beam



$$\text{Mean Dose} \approx \frac{(2r \cdot 2R - \pi r^2) \cdot \text{Target Height} \cdot D_r}{\text{Normal Tissue Volume}}$$

3A

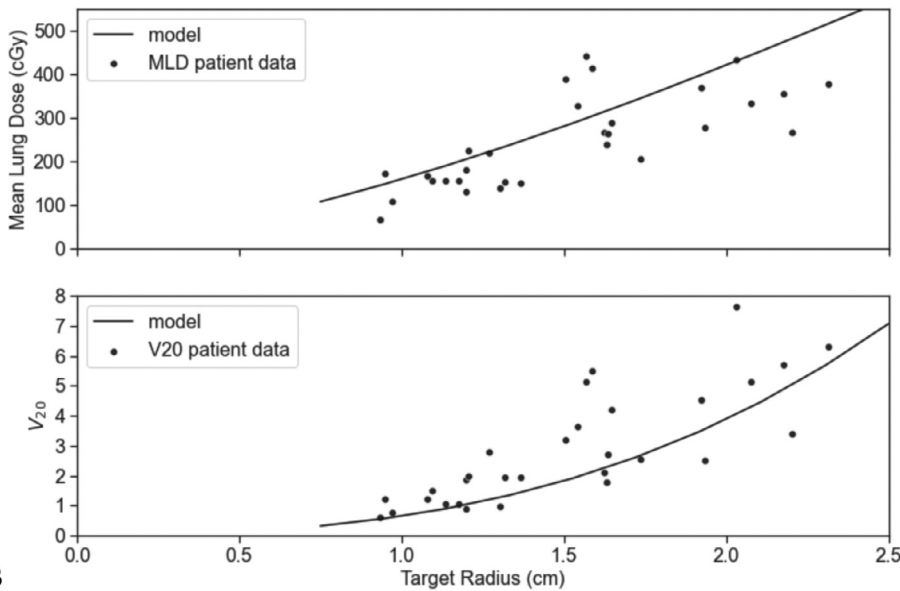


Fig. 3 A, On the left, an idealized 3-dimensional (3D) representation of a cylindrical target within a cylindrical normal tissue being treated with an axial arc. The percentage of normal-tissue volume at dose $\geq D_L$ can be computed as shown (essentially rearranging the equations in the prior figures; derivation in Appendix 2). On the right, the mean dose to the normal organ can be estimated as shown (for the setting of a single-treatment beam orientation). The mean dose is relatively stable irrespective of the number of beam orientations, as suggested by the cartoon on the top of Figure 2 A and formally demonstrated by others.¹³⁻¹⁵ B, C, The solid lines are from the idealized 3D model-based calculations of the predicted mean lung dose and V_{20} for targets with variable radii from 0.75 to 2.5 cm. These are highly correlated with the clinical data from the center of 1 of the authors (dots in B and C). The fit between the idealized model and the clinical data are clearly imperfect. Nevertheless, it is interesting that a simple model can provide reasonable estimates of clinical data. Further details are provided and discussed in Appendix E2.

orientations are used, intermediate doses will still be delivered in areas where the beams overlap. The sizes of these areas of overlap (again analogous to $V_{\geq 5}$, $V_{\geq 10}$, or $V_{\geq 20}$), are highly dependent on beam orientations, and

can fluctuate widely with beam number (see Appendix E1 for examples).

Nevertheless, with large numbers of beam orientations, these intermediate $V_{\geq x}$ values typically will stabilize. For

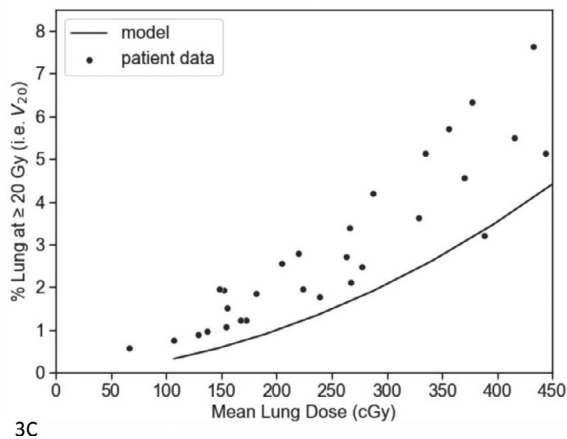


Fig. 3 Continued.

example, a full arc rotation in the simple 2D case leads to circular isodose lines, with doses (relative to the target dose) and radii (relative to the target radius) showing a simple relationship (Fig 2 B and 2 C). This can provide planners with some a priori estimate of the relative dose to nearby normal structures based on its distance from the target center relative to the target radius, for simple unoptimized or unmodulated arcs. Because the mean dose is essentially constant irrespective of beams and technique (as suggested by the cartoon on the top of Figure 2 A, formally demonstrated by others¹³⁻¹⁵ and further discussed in Appendix E1), a stabilizing value for $Area_{\geq x}$ (ie, area at dose $\geq x$) makes $Area_{\geq x}$ highly correlated with the mean dose. Thus, with the large number of beam orientations commonly used with SBRT/SRS, $V_{\geq x}$ and the mean dose will tend to be highly correlated with each other.

This idealized 2D representation can be readily expanded to a similarly idealized 3D representation of a cylindrical target (analogous to a lung lesion with respiratory excursion superiorly/inferiorly) within a cylindrical lung, treated with a set of beams orthogonal to the long axis of the cylinder (analogous to an axial arc-based treatment) (Fig 3). Interestingly, using a set of reasonable assumptions applied to the idealized model, one can compute estimates of $V_{\geq 20}$ and mean lung doses for axial treatments of small lung nodules that are similar to clinical data in patients treated using axial-like beams (Fig 3 and Appendix E2). We recognize that the assumption to ignore divergence and attenuation is not ideal, but these effects are modest.

In summary, the limited dose-response data for regional injury for some organs, such as the lung and parotid, provide some physiological rationale that may explain the predictive value of the mean dose. However, depending on the steepness of the dose-response function and the incidental doses delivered to the organ at risk, $V_{\geq x}$ values may be physiologically rational as well.

Further, there appear to be basic geometric principles that may drive a strong correlation between the mean dose and $V_{\geq x}$. Thus, from a pragmatic clinical-utility perspective, both the mean dose and $V_{\geq x}$ can be useful. Additional work is needed to better define dose-response functions for regional injury that may help to define optimal dosimetric predictors for global toxicity in parallel-like organs. However, the geometric realities predict high correlations between many of the commonly used dosimetric parameters (which are indeed seen in clinical data), and these correlations challenge our ability to assess their relative utility in predicting normal-tissue injury.

Acknowledgements

Because this work grew out of the HyTEC initiative, we acknowledge the support of the American Association of Physicists in Medicine for the HyTEC project.

Supplementary materials

Supplementary material associated with this article can be found in the online version at [doi:10.1016/j.adro.2022.101039](https://doi.org/10.1016/j.adro.2022.101039).

References

1. Marks LB, Yorke ED, Jackson A, et al. Use of normal tissue complication probability models in the clinic. *Int J Radiat Oncol Biol Phys.* 2010;76(3 suppl):S10–S19.
2. Grimm J, Marks LB, Jackson A, et al. High Dose per fraction, hypofractionated treatment effects in the clinic (HyTEC): An overview. *Int J Radiat Oncol Biol Phys.* 2021;110:1–10.
3. Briere TM, Agrusa JE, Martel MK, et al. Acute and late pulmonary effects after radiation therapy in childhood cancer survivors: A PENTEC comprehensive review [e-pub ahead of print]. *Int J Radiat Oncol Biol Phys.* <https://doi.org/10.1016/j.ijrobp.2022.01.052>, accessed August 23, 2022.
4. Bates JE, Keshavarz H, Rancati T, et al. Cardiac disease in childhood cancer survivors treated with radiotherapy: A systematic review. *Int J Radiat Oncol Biol Phys.* Submitted.
5. Milgrom SA, van Luijk P, Pino R, et al. Salivary and dental complications in childhood cancer survivors treated with radiation therapy to the head and neck: A pediatric normal tissue effects in the clinic (PENTEC) comprehensive review. In press.
6. Fried DV, Das SK, Marks LB. Imaging radiation-induced normal tissue injury to quantify regional dose response. *Semin Radiat Oncol.* 2017;27:325–331.
7. Marks LB, Munley MT, Spencer DP, et al. Quantification of radiation-induced regional lung injury with perfusion imaging. *Int J Radiat Oncol Biol Phys.* 1997;38:399–409.
8. Theuvs JC, Seppenwoolde Y, Kwa SL, et al. Changes in local pulmonary injury up to 48 months after irradiation for lymphoma and breast cancer. *Int J Radiat Oncol Biol Phys.* 2000;47:1201–1208.
9. Scheenstra AE, Rossi MM, Belderbos JS, et al. Local dose-effect relations for lung perfusion post stereotactic body radiotherapy. *Radiother Oncol.* 2013;107:398–402.

10. Buus S, Grau C, Munk OL, et al. Individual radiation response of parotid glands investigated by dynamic ^{11}C -methionine PET. *Radiother Oncol.* 2006;78:262–269.
11. Cao Y, Platt JF, Francis IR, et al. The prediction of radiation-induced liver dysfunction using a local dose and regional venous perfusion model. *Med Phys.* 2007;34:604–612.
12. Hope AJ, Lindsay PE, El Naqa I, et al. Modeling radiation pneumonitis risk with clinical, dosimetric, and spatial parameters. *Int J Radiat Oncol Biol Phys.* 2006;65:112–124.
13. Chapet O, Fraass BA, Ten Haken RK. Multiple fields may offer better esophagus sparing without increased probability of lung toxicity in optimized IMRT of lung tumors. *Int J Radiat Oncol Biol Phys.* 2006;65:255–625.
14. Reese AS, Das SK, Curie C, et al. Integral dose conservation in radiotherapy. *Med Phys.* 2009;36:734–740.
15. Fitzgerald R, Owen R, Barry T, et al. The effect of beam arrangements and the impact of non-coplanar beams on the treatment planning of stereotactic ablative radiation therapy for early stage lung cancer. *J Med Radiat Sci.* 2016;63:31–40.